woodlands (*19*), the Mexican domesticates and the Russell Cave fruits (*18*) fall within the size range of modern wild varieties of the genus. Both the Mexican domesticated forms of *Chenopodium* and the Russell Cave fruits, however, have a greater internal fruit volume and more perisperm than do wild fruits of the same diameter because of the shift to a rectanguloid cross section. A total of 387 Russell Cave *Chenopodium* fruits were sufficiently intact to enable observation of cross-section and margin configuration, with 353 (92 percent) having a rectanguloid cross section and truncate margin.

The Russell Cave *Chenopodium* assemblage exhibits a set of interrelated morphological characteristics that reflect domestication and establish the presence of a domestic variety of the species *Chenopodium berlandieri* within the garden plots of the eastern woodlands by 2000 years ago. Whether this early domesticate was introduced from Mexico or was the product of an independent process of domestication is not known.

BRUCE D. SMITH
Department of Anthropology,
National Museum of Natural History,
Smithsonian Institution,
Washington, D.C. 20560

References and Notes

1. R. Yarnell, "Prehistoric plant foods and husbandry in eastern North America," paper presented at the 48th annual meeting of the Society for American Archaeology, Pittsburgh, 29 April 1983.
2. M. Kay, F. B. King, C. K. Robinson, *Am. Antiq.* **45**, 806 (1980).
3. N. Conard, D. Asch, N. Asch, D. Elmore, H. Grove, M. Rubin, J. Brown, M. Wiant, K. Farnsworth, T. Cook, *Nature (London)*, in press.
4. D. Asch and N. Asch, "A chronology for the development of prehistoric horticulture in west central Illinois," paper presented at the 47th annual meeting of the Society for American Archaeology, Minneapolis, 17 April 1982.
5. D. Asch and N. Asch, in *Cent. Am. Archeol. Contract Archeol. Program Rep. Invest.* **137** (1983).
6. S. Johannessen, in *American Bottom Archaeology*, C. Bareis and J. Porter, Eds. (Univ. of Illinois Press, Urbana, 1984).
7. D. Asch and N. Asch, *Mid-Cont. J. Archaeol.* **2**, 3 (1977).
8. H. D. Wilson, *Econ. Bot.* **35**, 233 (1981).
9. G. Fritz, *Am. Antiq.* **49**, 558 (1984).
10. J. R. Harlan, J. M. J. de Wet, E. G. Price, *Evolution* **27**, 311 (1973).
11. H. D. Wilson and C. B. Heiser, Jr., *Am. J. Bot.* **66**, 198 (1979).
12. H. D. Wilson, *Syst. Bot.* **5**, 253 (1980).
13. ______, *ibid.* **6**, 253 (1981).
14. J. Griffin, *Pub. Archaeol.* **13** (No. 13) (1974).
15. C. Miller, *Natl. Geogr.* **110**, 542 (1956).
16. ______, *ibid.* **113**, 426 (1958).
17. ______, *South. Indian Stud.* **14**, 31 (1960).
18. Russell Cave is located south of the present-day range of *C. bushianum* and north of the known range of *C. berlandieri*. With a mean fruit diameter of 1.33 mm ($n = 525$; range, 1.0 to 1.8 mm, standard deviation 0.13), however, the Russell Cave assemblage compares favorably with *C. berlandieri* and not with the larger fruited *C. bushianum* (*7*). See Wilson (*12*) for a discussion of the probable conspecific nature of *C. bushianum* and *C. berlandieri*.
19. R. Yarnell, in *Univ. Mich. Mus. Anthropol. Anthropol. Pap.* **67** (1978), p. 289.

5 March 1984; accepted 24 July 1984

Venus: Volcanism and Rift Formation in Beta Regio

Abstract. *A new high-resolution radar image of Beta Regio, a Venus highland area, confirms the presence of a major tectonic rift system and associated volcanic activity. The lack of identifiable impact craters, together with the apparent superposition of the Theia Mons volcanic structure on the rift system, suggest that at least some of the volcanic activity occurred in relatively recent geologic time. The presence of topographically similar highland areas elsewhere on Venus (Aphrodite Terra, Dali Chasma, and Diana Chasma) suggests that rifting and volcanism are significant processes on Venus.*

Among the terrestrial planets and satellites, Venus is the most like the earth in size and density and may provide important clues to planetary thermal and tectonic evolution (*1, 2*). The nature of the geologic processes that form and modify the surface of Venus are poorly known, however. The atmosphere of Venus precludes observations of the surface at visible wavelengths from orbit. Radar observations, however, have provided information about the general topography (*3, 4*) and more detailed images of parts of the surface (*5–7*). This information has revealed the presence of highland regions on Venus rising more than 1.5 km above mean planetary radius and comprising about 8 percent of the surface of the planet (*4*). Establishing the nature and origin of these highland regions is critical to deciphering the geologic history of the planet and to understanding the mechanisms of lithospheric heat transfer (*2*). We describe new high-resolution radar images of the Beta Regio highlands of Venus that show details of volcanic and tectonic features and provide insight into the formation of highlands on Venus.

Beta Regio is an oval-shaped highland region centered near 25°N latitude and 280° longitude. It extends for about 2500 km in a north-south direction and is approximately 2000 km wide, rising as high as 5 km above median radius (Fig. 1, a and b). Early radar observations of Venus from the earth (*6, 8*) revealed the presence of two radar-bright features in this region that were designated Beta (now called Theia) and Delta (now Rhea). Subsequent data revealed more details of these features (*5, 9, 10*) and provided topographic information, leading Saunders and Malin (*11*) to characterize Theia as an elevated, high-reflectivity region approximately 700 km across, with a summit region rising 10 km above its surroundings. In the center of the summit there was a low-reflectivity region, 60 to 90 km in diameter. Saunders and Malin interpreted Theia and Rhea to be large volcanic constructs similar to those of the Tharsis region of Mars. Additional images made from the earth at 10 km resolution (*12*) and Pioneer-Venus altimetry, roughness, and reflectivity measurements (*3, 4*) allowed further characterization. Masursky *et al.* (*4*) noted that Beta Regio has complexly varying radar brightness values, elevations, and root-mean-square slopes. The two irregularly shaped shieldlike features Theia and Rhea Montes dominate the topography (Fig. 1, a and b) and lie adjacent to a central north-south trending canyon (*13, 4*), which appears to be a northern extension of a complex disrupted region of en echelon (parallel but each offset to the front or rear) ridges and troughs south of Beta Regio. Masursky *et al.* (*4*) interpret the central Beta Regio trough to be a rift and Rhea and Theia Montes to be constructional volcanic features. McGill *et al.* (*14*) have drawn topographic analogies between Beta Regio and the East African rift system.

In August and September 1983, we obtained a high-resolution image (approximately 2 km radar resolution) (Fig. 1a) of central Beta Regio that reveals geologic details of Rhea and Theia Montes and the central chasma. The image was obtained with the 12.6-cm wavelength radar system at Arecibo Observatory in Puerto Rico. The image maps the backscatter cross section per unit area (surface reflectivity) with the angle at which the surface is illuminated by the incident radar wave varying across the image from approximately 44° to 52°. Scattering laws and the data acquisition and reduction techniques are described elsewhere (*5*). In this image, variations in brightness are mainly due to differences in small-scale (wavelength-size) surface roughness (bright, high values, and dark, low values), but variations in the surface dielectric constant also play a role. For some of the linear features in the region between Theia and Rhea Montes there is evidence for single-scatter quasispecular reflection indicating the presence of steep slopes.

The high-resolution image (Fig. 1a) shows four distinctive regions. Along the eastern side of the image are a series of parallel to subparallel bright linear features forming a zone 100 to 350 km in width. This zone corresponds to the linear topographic depression or central trough in the profiles of Fig. 1b. There are two bright regions: a circular feature in the south about 350 km in diameter corresponds to Theia Mons, and a diffuse but bright area straddling the chasm in the north. The brightest area adjacent to the chasm on the western side corresponds to Rhea Mons. The western portion of the image is characterized by relatively low but variable backscatter and lacks the prominent patterns noted in the central and eastern areas.

The distribution of bright and dark linear features is shown in Fig. 1c. Most are 25 to 100 km long but some range up to several hundred km in length. They are arranged with the long axes parallel to subparallel, trending north to northeast, and many are arranged in en echelon patterns. The distribution of the linear features is closely related to the central topographic depression. On the basis of these characteristics, the linear features are interpreted to be areas of enhanced roughness, or very steep slopes associated with faults, or both, and this collection of faults related to the central depression are interpreted to be a rift system as suggested previously on the basis of topographic data (*11*, *14*).

The topography and radar image (Fig. 1, a to c) reveals much about the details of the chasma (a central depression) rift system. At the northern end of the image, the rift is approximately 350 km wide and appears to be diverging toward the north into two segments (Fig. 1b, profile A-A′). Over the next 400 to 500 km to the south, the rift zone narrows to 100 to 200 km, and faulting is concentrated in a central depression between Rhea Mons on the western rim and a radar-bright structure on the eastern rim (Fig. 1b profiles B to E). The bright lines interpreted to be faults are closely spaced in this region, averaging 10 to 20 km apart, and they extend for distances of 25 to 150 km along the strike of the valley. At the southern end of this region (profile F) the rift structure widens to 250 km, individual lines become locally more prominent, but the chasma topography is shallow.

Between profile F and Theia Mons, a distance of 500 to 700 km, the topography of the chasma becomes complex. The rift structure (profile G) is wide (250 km) relative to the topographic depression to the north and the depression has a different orientation and appears to be offset slightly toward the east. The change in orientation of the depression (trending more northeasterly) is accompanied by a similar change in orientation of the strike of many of the faults (Figure 1, a to c).

Between profile G and Theia Mons (profiles H and I), two additional depressions are encountered and the rift structure widens to at least 300 km. In the vicinity of Theia Mons, the bright lines are strikingly less abundant, the chasmal topography is obscured, and the positive topography of Theia Mons dominates, suggesting that Theia Mons may be superposed on the chasm and relatively undisturbed by faulting. South of Theia Mons, the rift structure appears to diverge with the eastern arm becoming the prominent Devana Chasma and the western arm extending into the surrounding lowlands. Although there is a wide variation in brightness throughout the chasma region of central Beta (Fig. 1a), nonethe-

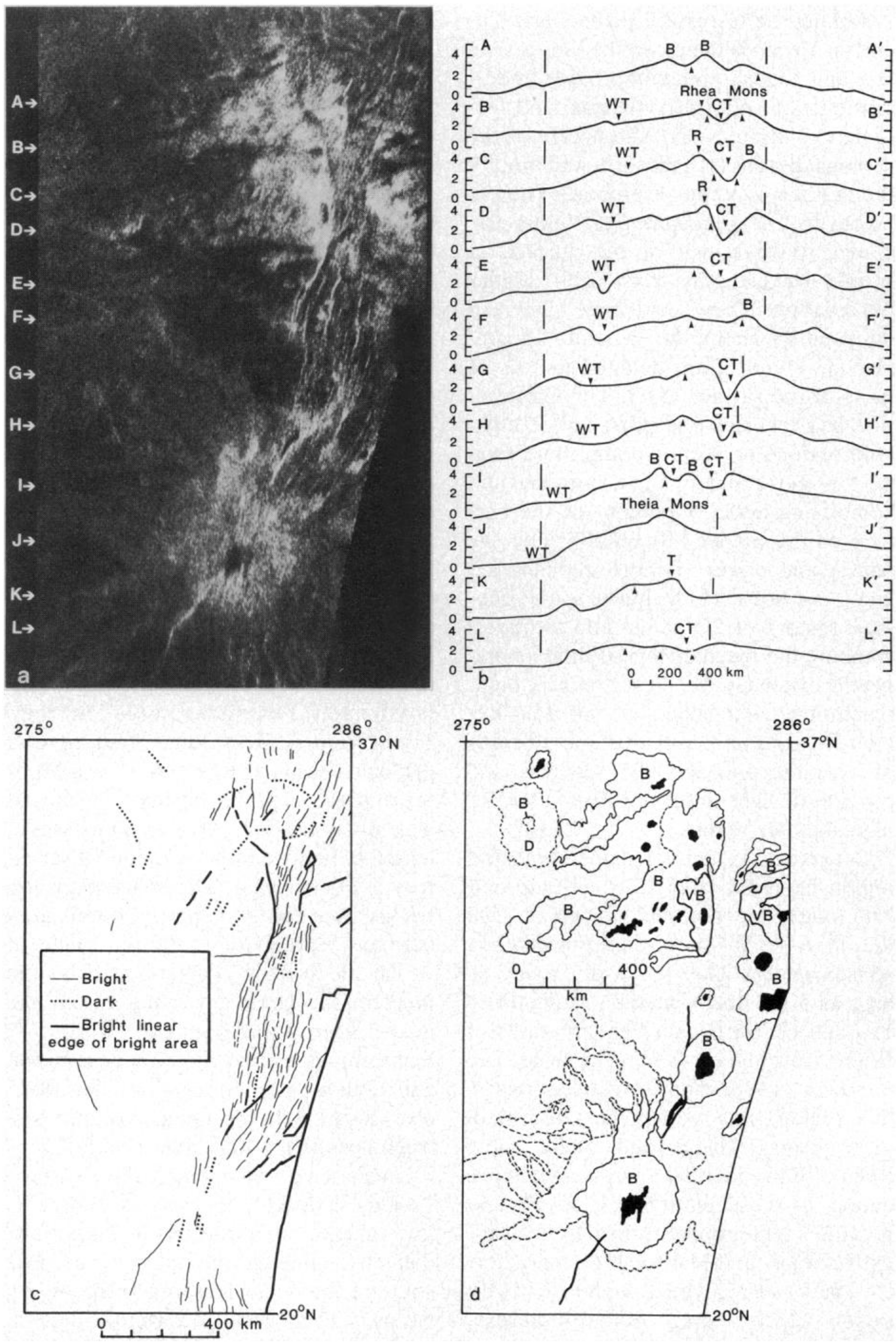

Fig. 1. (a) High resolution radar image of central Beta Regio. Resolution is approximately 2 km (*25*). Variations in brightness are related to differences in small-scale (wavelength-size) surface roughness values (darkest areas are smoothest and brightest areas are roughest). Letters indicate locations of profiles in (b). (b) Topographic profiles derived from Pioneer-Venus altimetry (*14*); datum is median radius, 6051.2 km. WT, western trough; CT, central trough; and B, bright area in (a). Vertical lines mark the location of the edge of the image (a). Vertical arrows mark the best estimate of the location of the major bounding faults. (c) Sketch map of bright and dark linear features in radar image. (d) Sketch map of bright areas (B) with central dark regions (black), lobate flowlike features, and a dark area (D) with a central bright region (B).

less several of the deep depressions are characterized by relatively low radar brightness.

Support for a volcanic origin for Theia Mons (*11, 14*) comes from its apparent superposition on the western bounding fault of the rift, the extremely close correlation of topography and the major brightness variation, and lobate flowlike features extending radially away from the central area for several hundred kilometers in a downslope direction (Fig. 1d). Theia Mons rises over 5 km above the datum and 1.5 to 2.5 km above the surrounding crest of Beta Regio (compare profiles G and J, Fig. 1b). A circular area of high radar backscatter and approximately 350 km in diameter is situated directly on the topographic high. A smaller and irregular region of low backscatter, 60 to 90 km in diameter is located approximately at the center of the bright area (Fig. 1, a and d). These two features are centered on the extension of the western edge of the rift system (Fig. 1), suggesting a correlation of the location of a prominent volcanic center and a major fault. The dark feature could be relatively smooth volcanic deposits, perhaps lava flows related to a central caldera region, as is common on terrestrial volcanoes. The bright spot represents a relatively rougher surface (combined with enhanced dielectric constant) and this region is interpreted as lava flows, which are responsible for the primary buildup of the volcano. The edge of this area is somewhat diffuse over an additional radial distance of 25 to 50 km. Toward the west and northwest this diffuseness merges into a series of lobate flowlike features extending for an additional 400 to 500 km (Fig. 1d). Although of very low contrast, these flowlike features are 25 to 75 km wide and trend generally downslope. They may represent sets of flows emanating from Theia Mons or additional vents along the rift. At the present resolution, establishing their nature and point of origin is difficult. Theia Mons interrupts the topography and structure of the rift system (Fig. 1, a to d), strongly suggesting that it is superposed on the rift structure and is therefore younger. Several bright and dark bands extend into the central part of Theia (Fig. 1c) and are parallel to the general trend of the trough, suggesting that some faulting may have occurred during or after the formation of Theia Mons.

The correlation of topography and variations in brightness on Theia Mons and the evidence suggesting that it represents a major shield volcano prompt the examination of other areas with similar characteristics. Figure 1d shows the location of several other areas with bright regions of various shapes and central dark spots that are often related to an elevated area. The most prominent of these, Rhea Mons, is located along the western edge of the rift system, rises 0.5 to 1.0 km above the surrounding terrain, but has a sharp boundary along its eastern margin, adjacent to one of the deeper portions of the rift (Fig. 1, a to d). Similarities to Theia Mons suggest a volcanic origin; however, the feature appears to be more extensively modified by rift faulting (Fig. 1c). The large number of these features and their relation to the rift valley suggest that extensive volcanism has accompanied rift formation in Beta Regio and that a significant portion of the rim topography of the rift may be locally due to the construction of volcanic edifices.

The topography of Beta and Phoebe Regio shows many similarities to continental rift systems on the earth (*14, 15*). The more detailed view of the chasma revealed by this image strengthens and extends this comparison and interpretation. Similarities include (i) association of a major rift system with the crest of a broad topographic high (*16*); (ii) a strong correlation of a central depression (a chasma) and bright linear features interpreted to be faults (Fig. 1, b and c); (iii) the parallel and en echelon nature of the fault systems (*17*); (iv) the change in orientation of the rift system every several hundred kilometers (*18*); (v) changes in depth along strike; (vi) the presence of volcanic constructs in association with the rift system; and (vii) the association of several volcanic constructs with bounding faults of the rift system (*19*). Convective thinning of the lithosphere could produce uplift leading to rifting and volcanism on Venus. Comparison of Beta regional topography and components related to volcanic construction (Fig. 1) will permit refinement of the models for Venus rift formation (*20, 21*).

It has been proposed that the Beta region may be the site of present-day explosive volcanic eruptions (*22*). Our data confirm the presence of flows and volcanic constructs and suggest that some volcanic deposits (Theia Mons) postdate much of the faulting in the rift. These observations, combined with an apparent lack of large impact craters, suggest a relatively young geologic age. Comparison of this image with lower resolution images obtained several years ago shows no evidence for major surface changes. Our data do not, however, allow us to establish or rule out very recent volcanic activity. Environmental conditions influence the style of volcanism on the planets (*23*) and on Venus the present high surface atmospheric pressure means that explosive volcanic eruptions are likely to be uncommon unless magma volatile contents are much higher than commonly observed on the earth. The relatively rough deposits surrounding Theia Mons suggest the presence of flow deposits rather than relatively smoother surfaces typical of pyroclastic airfall deposits. However, higher resolution images are required so that individual flow features can be mapped and the presence or absence of pyroclastic volcanism can be established.

Schaber (*24*) has pointed out the global distribution of chasmata on Venus and has suggested that they represent global rift systems comparable to continental-type rifts of the earth. The new information on the nature of rift formation on Venus and the nature and rôle of volcanism in this process obtained from our data indicates that rift formation and associated volcanism are important processes on Venus and that they contribute significantly to the formation and evolution of highland areas such as Beta Regio. Other areas, such as Aphrodite Terra, where topographically similar chasma (Dali, Diana) are abundant (*3, 4, 24*), may also have a similar origin.

D. B. CAMPBELL

National Astronomy and Ionosphere Center, Arecibo Observatory, Arecibo, Puerto Rico 00612

J. W. HEAD

Department of Geological Sciences, Brown University, Providence, Rhode Island 02912

J. K. HARMON
A. A. HINE

National Astromony and *Ionosphere Center, Arecibo Observatory*

References and Notes

1. J. W. Head and S. C. Solomon, *Science* **213**, 62 (1981).
2. S. C. Solomon and J. W. Head, *J. Geophys. Res.* **87**, 9236 (1982).
3. G. H. Pettengill *et al.*, *ibid.* **85**, 8261 (1980); G. H. Pettengill *et al.*, *Science* **217**, 640 (1982); P. G. Ford and G. H. Pettengill, *ibid.* **220**, 1379 (1983).
4. H. Masursky *et al.*, *J. Geophys. Res.* **87**, 8232 (1980).
5. D. B. Campbell and B. Burns, *ibid.*, p. 8271.
6. R. M. Goldstein, *Radio Science* **69D**, 1623 (1965).
7. D. B. Campbell *et al.*, *Science* **193**, 1123 (1976).
8. S. Zohar and R. M. Goldstein, *Astron. J.* **79**, 85 (1974).
9. R. M. Goldstein and H. C. Rumsey, *Science* **169**, 974 (1970); *Icarus* **17**, 699 (1972).
10. H. C. Rumsey *et al.*, *Icarus* **23**, 1 (1974).
11. R. S. Saunders and M. C. Malin, *Geophys. Res. Lett.* **4**, 547 (1977); M. C. Malin and R. S. Saunders, *Science* **196**, 987 (1977).
12. D. B. Campbell *et al.*, *Science* **204**, 1424 (1979).
13. R. M. Goldstein *et al.*, *J. Geophys. Res.* **81**, 4807 (1976).
14. G. E. McGill *et al.*, *Geophys. Res. Lett.* **8**, 737 (1981).
15. C. A. Wood and J. W. Head, in *Tectonics and*

Geophysics of Continental Rifts, B. Ramberg and E. R. Neumann, Eds. (Reidel, Dordrecht, Netherlands, 1978), p. 401.
16. M. H. P. Bott, *Tectonophysics* **73**, 1 (1981).
17. R. W. Girdler, *ibid.* **94**, 241 (1983).
18. C. A. Wood, *ibid.*, p. 529.
19. L. A. J. Williams, in *Continental and Oceanic Rifts, Geodynamics Series*, G. Palmason, Ed. (American Geophysical Union, Washington, D.C., 1982), vol. 8, p. 193.
20. S. C. Solomon and J. W. Head, *Lunar Planet. Sci.* **15**, 806 (1984).
21. T. Spohn and G. Schubert, *Tectonophysics* **94**, 67 (1983).
22. F. L. Scarf and C. T. Russell, *Geophys. Res. Lett.* **10**, 1192 (1983); L. W. Esposito, *Science* **223**, 1072 (1984).
23. C. A. Wood, *NASA Tech. Memo TM-80339* (1979), p. 244; J. W. Head and L. Wilson, *Lunar Planet. Sci.* **13**, 312 (1982); J. B. Garvin *et al.*, *Icarus* **52**, 354 (1982).
24. G. G. Schaber, *Geophys. Res. Lett.* **9**, 499 (1982).
25. The 2-km resolution is defined in terms of the ambiguity function of the radar system (5). Line pair resolution would be approximately 4 km.
26. We thank the staff of the Arecibo Observatory for assistance in data collection; the National Astronomy and Ionosphere Center is operated by Cornell University under contract with NSF and with support from NASA. Supported in part by NASA grant NGR-40-002-088 to J.W.H.

30 April 1984; accepted 1 August 1984

Increased Stratospheric Hydrogen Chloride in the El Chichón Cloud

Abstract. *Spectroscopic observations of the total column amount of hydrogen chloride above an altitude of 12 kilometers in the latitude range 20° to 40°N have been made both before and 3 to 6 months after the eruptions of El Chichón Volcano in March and April 1982. In the region of the cloud of volcanic aerosols, the hydrogen chloride total column after the eruptions increased by approximately 40 percent, even after allowance is made for the global secular increase in hydrogen chloride of 5 percent per year. The column amounts of hydrogen fluoride show no such increase.*

The family of odd-chlorine species, that is, Cl, ClO, HCl, HOCl, and $ClONO_2$, is important in stratospheric chemistry because of the potential of Cl and ClO to catalyze the removal of O_3 (*1*). Hydrogen chloride serves both as a temporary reservoir for chlorine, from which Cl can be released by reaction with OH, and as the ultimate sink for stratospheric chlorine by diffusion to the troposphere and rainout. It is believed that the principal source of stratospheric chlorine is diffusion of chlorofluoromethanes from the troposphere (*2*); the discovery of additional natural sources of chlorine in the stratosphere could modify our understanding of the chemistry of the O_3 layer.

Recently Mankin and Coffey (*3*) reported spectroscopic measurements of the total column amount of HCl and HF above their 12-km observation height as a function of latitude and time. Data in mid-latitudes, covering 5 years, indicate a rate of increase of stratospheric HCl of about 5 percent per year.

In March and April 1982, there were major eruptions of El Chichón Volcano (17°N, 93°W) in Mexico. The volcano injected large amounts of gas and particles into the lower stratosphere (*4*). A coherent cloud was soon established in a zonal band circling the earth (*5*). There have been numerous reports of ensuing changes in the stratospheric sulfur chemistry (*6*), the aerosol burden (*7*), and the visible and infrared optical depths of the stratosphere (*8*), as well as changes in stratospheric chlorine (*9*) and NO_2 (*10*).

In July through October 1982, we observed the infrared transmission spectrum of the stratosphere near the northern edge of the cloud of debris from El Chichón. We flew a high-resolution Fourier-transform spectrometer aboard the National Center for Atmospheric Research Sabreliner jet aircraft to measure the spectrum of sunlight that has passed through the upper atmosphere. Analysis of the absorption spectra allows quantitative determination of the total amount of numerous trace species in the atmosphere above the aircraft. Spectra were recorded from 2.5 to 13 μm with an apodized spectral resolution of 0.06 cm^{-1}. The instrumentation and technique are discussed in detail elsewhere (*11*).

By September 1982, the cloud of gas and particles from the volcano had spread zonally around the globe and extended in latitude from 10°S to 35°N, as shown in lidar and satellite observations (*12*). We made two flights in early July 1982 and seven more between 15 September and 1 October 1982. The flights were made along a constant-pressure surface of 198 mbar (~11.9 km altitude) along the paths shown in Fig. 1.

Individual spectra were recorded in 6 seconds; spectra were averaged in groups of five or ten to improve the signal-to-noise ratio before analysis. A small portion of one of the averaged spectra is shown in Fig. 2b; a similar spectrum recorded in 1978, before the El Chichón eruptions, is shown in Fig. 2a. The small differences in the spectra are attributable to noise and to a slow wandering of the background level caused by aircraft vibration. The difference in absorption in the HCl line between the two spectra is dramatic. We analyzed the spectra for HCl by comparing the observed spectra with synthetic spectra calculated from the line parameters in the Air Force Geophysics Laboratory compilations (*13*), using the R_1 and R_2 lines of the $H^{35}Cl$ fundamental band. Other species used in the synthetic spectra include water vapor, O_3, and CH_4; sulfur gases such as SO_2, which might be enhanced in the cloud, do not absorb in this spectral region. The depth of the line in the observed spectrum was compared with the depth of the same line in the calculated spectrum for various amounts of HCl in the calculation. The greatest uncertainty is in the subjective determination of the background level from which to measure the depth. The analysis procedure and the line parameters used were the same as in our earlier work (*3*). The column amounts from dif-

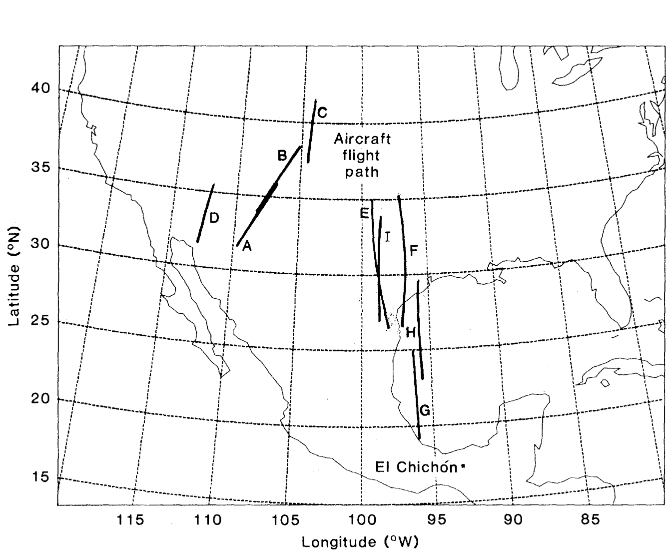

Fig. 1. Map showing the paths of flights made in July through October 1982. Dates for individual flights are given in Table 1. The letter plotted beside each flight path indicates the corresponding entry in Table 1.